ARMY RESEARCH LABORATORY

Wide Bandgap Transit Time Devices for Achieving High Frequency Operation

Richard H. Wittstruck

ARL-TR-1125 October 1996

APPROVED FOR PUBLIC RELEASE; DISTRIBUTION IS UNLIMITED.

NOTICES

Disclaimers

REPORT DOCUMENTATION PAGE		Form Approved OMB No. 0704-0188

1. AGENCY USE ONLY *(Leave blank)*

2. REPORT DATE
October 1996

3. REPORT TYPE AND DATES COVERED
Technical Report

4. TITLE AND SUBTITLE
Wide Bandgap Transit Time Devices for Achieving High Frequency Operation

5. FUNDING NUMBERS

6. AUTHOR(S)

Richard H. Wittstruck

7. PERFORMING ORGANIZATION NAME(S) AND ADDRESS(ES)
US Army Research Laboratory (ARL)
Physical Sciences Directorate
ATTN: AMSRL-PS-DE
Fort Monmouth, NJ 07703-5601

8. PERFORMING ORGANIZATION REPORT NUMBER

ARL-TR-1125

9. SPONSORING/MONITORING AGENCY NAME(S) AND ADDRESS(ES)

10. SPONSORING/MONITORING AGENCY REPORT NUMBER

11. SUPPLEMENTARY NOTES

12a. DISTRIBUTION/AVAILABILITY STATEMENT

Approved for Public Release: Distribution is Unlimited

12b. DISTRIBUTION CODE

13. ABSTRACT *(Maximum 200 words)*

The proposed device described offers a simple method for achieving the generation of high frequency signals. More particularly, the device pertains to achieving high frequency signals using semiconductor materials having increased electron saturation velocity over those values for gallium arsenide (GaAs) and silicon (Si). The use of such materials, together with submicron scale and nano-scale device processing techniques, affords devices having frequencies up to and including the terahertz band with high temperature and radiation hard characteristics. Such devices include transit-time-based oscillators for use in military and civilian radar receivers, logic devices, burglar/proximity alarm systems, biological/ chemical agent detectors and secure communications modules.

14. SUBJECT TERMS

BARITT, terahertz, wide bandgap semiconductor

15. NUMBER OF PAGES
15

16. PRICE CODE

17. SECURITY CLASSIFICATION OF REPORT	18. SECURITY CLASSIFICATION OF THIS PAGE	19. SECURITY CLASSIFICATION OF ABSTRACT	20. LIMITATION OF ABSTRACT
Unclassified	Unclassified	Unclassified	UL

NSN 7540-01-280-5500

Standard Form 298 (Rev. 2-89)
Prescribed by ANSI Std. 239-8
298-01

TABLE OF CONTENTS

LIST OF FIGURES

LIST OF TABLES

1.0 INTRODUCTION

It is known in the art of microwave generation that transit-time, transferred electron and field effect transistor devices are efficient sources of microwave energy.

Large signal behavior of transit-time devices was postulated in the late 1960's, and Si and GaAs devices based on this theory were demonstrated in the late 1970's and early 1980's and have been more fully described in such treatises as References 1 and 11.

The fundamental features common to these devices are the direct proportionality between the operating frequency and saturation velocity, and the inverse proportionality between frequency and depletion region width.

Specific examples of these transit time devices are IMPATT (impact ionization avalanche and transit time) diodes and BARITT (barrier injected transit time) diodes. IMPATT and BARITT diodes are typically used as devices which amplify high frequency waves into high power waves or generate an oscillation of high frequency waves with high power.

IMPATT diodes typically include an n+ type (or p+ type) semiconductor layer, an n-type (or p-type) semiconductor layer and a p+ type (or n+ type) semiconductor layer, all of which make a strata in this order. Electrodes are fitted on both ends (n+ type and p+ type of layers) of the strata. In operation, a reverse bias voltage is applied to the diode; that is, the electrode of the n+ type layer is connected to the positive terminal of an electric power source, and the electrode of the p+ type layer is connected to the negative terminal of the power source. This reverse bias voltage induces a carrier avalanche in the less doped semiconductor layer (i.e., the n-type layer). The electrons generated by the avalanche run through the less doped semiconductor layer to the n+ type layer with saturated velocity. This phenomenon induces negative resistance in the diode. The occurrence of negative resistance enables the diode to generate microwave oscillation. A typical IMPATT diode has a pn-junction. But there are other types of IMPATT diodes in which the pn-junction is replaced by a Schottky junction between a metal and a semiconductor.

BARITT diodes typically have a structure in which a metal layer, an n-type layer (or p-type layer) of semiconductors and a metal layer make strata in this order (i.e., Fig. 1). One type of junction between the metal and one semiconductor layer is a Schottky junction. Similar to IMPATT diodes, when a bias voltage is applied to the diode, minority carriers are injected to the semiconductor layer. The action of the minority carriers generates microwave oscillation. Also, like IMPATT diodes, BARITT diodes

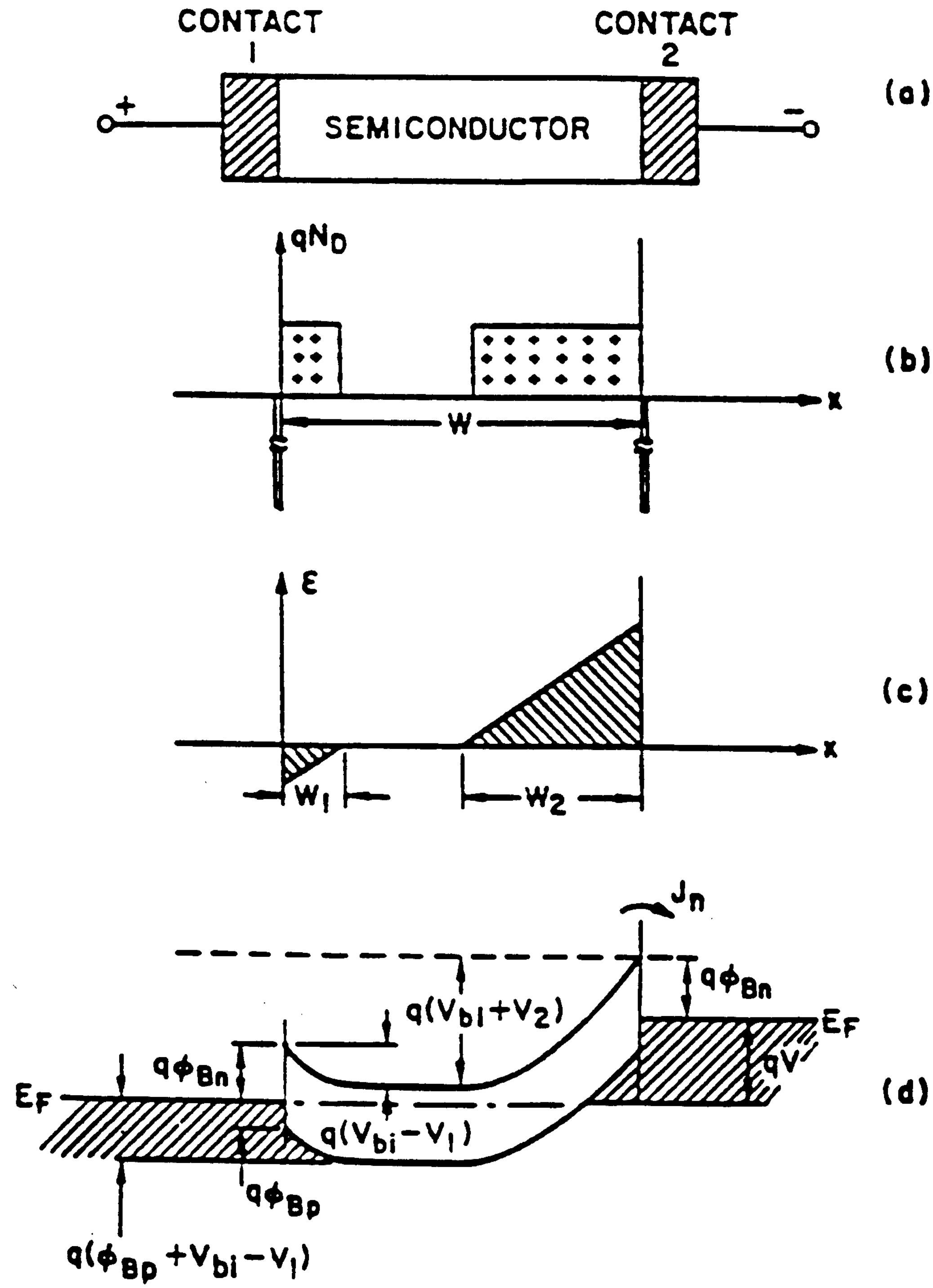

Figure 1 Metal–semiconductor–metal (MSM) structure. (*a*) MSM with a uniformly doped *n*-type semiconductor. (*b*) Charge distribution under low bias. (*c*) Field distribution. (*d*) Energy-band diagram.

can have a pn-junction instead of the Schottky junction between the metal and the semiconductor.

In the past, silicon or gallium arsenide have been the semiconductor material of these high frequency devices (IMPATT and BARITT diodes). Other semiconductor materials have not been used as the material of choice for these high frequency devices so far, although diamond has been shown to lower the heat in such transit time devices based on silicon and gallium arsenide. Such a device made from diamond is disclosed in U.S. Patent No. 5,243,119, issued to Shiomi et al. on September 7, 1993. Unfortunately, known transit-time oscillator devices based on silicon and gallium arsenide are, at best, capable of generating only gigahertz range frequency signals. Therefore, it would be desirable to produce transit-time oscillator devices capable of generating terahertz range frequency signals.

With the advent of new material systems, such as III-nitrides and carbides, new opportunities arise for revisiting the mature transit time theory and deriving a new generation of transit time devices capable of terahertz frequency generation.

2.0 DEVICE DESCRIPTION

Using Hermann-Mauguin notation, $\bar{4}3m$ and 6mm crystallographic point group member material (and associated alloys thereof), could constitute a device capable of high frequency operation. The principal parameters for such performance advancements are the increased electron saturation velocities (in excess of $2 \times 10^{+7}$ cm/s) of some members of these crystal groups coupled with the use of submicron device processing yielding depletion regions of approximately 10^{-7} m. By using these materials and processes, transit time devices may be fabricated that are capable of generating terahertz frequency signals.

Additionally, in using these materials, their crystalline structure, with its intrinsic wide energy band gap (>2eV), will make these devices relatively impervious to irradiation. Moreover, the high thermal conductivity (5-20 watts/cm°K) of these materials affords device operation in high ambient temperature environments. Therefore, the proposed structure provides an improved class of devices, such as IMPATT and BARITT devices, which achieve high temperature, high frequency, radiation-hard operation.

The proposed device can be configured in any number of configurations, such as MSM, p-n-i-p, p-n-p and p-n-metal structures. Specifically, the device provides a transit-time oscillator which includes a substrate of semi-insulating material or semi-conducting material of a first conductivity type; a buffer layer on the substrate

comprising a material selected from the group consisting of $\bar{4}3m$ and 6mm crystallographic point group members, and alloys thereof, which have a high doping of a second conductivity type; an epitaxial layer on the buffer layer comprising a material selected from the group consisting of $\bar{4}3m$ and 6mm crystallographic point group members, and alloys thereof, which have a doping of a second conductivity type in an amount different than the doping of the buffer layer; a first electrical contact on the epitaxial layer; and a second electrical contact on the buffer layer isolated from the epitaxial layer.

In operation, this transit time oscillator is forward biased with a direct current (D.C.) signal to the first electrical contact resulting in a reverse bias D.C. signal being applied to the second electrical contact, resulting in a negative resistance producing propagation of oscillation signals of high frequency.

The structure provides a single epitaxial layer, transit-time microwave oscillator device capable of generating signals up to and including the terahertz frequency range. Suitable substrate materials for such a structure may include silicon carbide, gallium nitride, gallium aluminum nitride, silicon, gallium phosphide, lithium metagalate, lithium meta-aluminate, sapphire, and scandium nitride. In the preferred embodiment, the buffer layer comprises a silicon carbide or Group III nitride semiconductor material having a high doping of a second conductivity type. Suitable materials for the buffer layer non-exclusively include binary, tertiary and quaternary Group III nitrides such as aluminum nitride, thallium nitride, boron nitride, indium nitride, indium gallium nitride, gallium nitride and aluminum gallium nitride.

On the buffer layer is an epitaxial layer, which also comprises the same type of semiconductor material as the buffer layer, and is doped with a different doping of a second conductivity type than the doping of the buffer layer.

In using these wide bandgap materials as the buffer and epitaxial layers, terahertz frequencies are now possible. Recall, this is true because the fundamental common relationship amongst these groups of devices is the direct proportionality between the operating frequency and the saturation velocity V_{sat}.

Another underpinning relation is the inverse proportionality between frequency and the depletion region width. Therefore, because these materials exhibit saturation velocities in excess of 2×10^7 cm/s coupled with submicron device processing which can yield depletion regions of approximately 10^{-7} m, the present device is capable of generating greater than terahertz frequencies.

These relationships, providing for this terahertz frequency capability, are shown mathematically through the following large signal behavior relation:

$$f = \frac{\theta_d V_{sat}}{L},$$

where θ_d is drift angle, L is the depletion region width, and V_{sat} is the saturation velocity.

In the most preferred embodiment, the buffer layer is heavily doped with an n+ type doping and the epitaxial layer is doped differently with an n type doping.

In this case, the substrate is a semi-insulating material or a semi-conducting material of the p conductivity type.

In an alternate embodiment, the buffer layer is heavily doped with a p^+ type doping and the epitaxial layer is doped differently with a p type doping. In this case, the substrate is a semi-insulating material or a semi-conducting material of the n conductivity type.

In either embodiment, the n^+ type or p^+ type doping of the buffer layer is linearly graded, in the lateral dimension, to the corresponding doping of the epitaxial layer in order to achieve low contact resistivity.

The buffer and the epitaxial layers are preferably grown on the substrate by molecular beam epitaxy or metal organic chemical vapor deposition techniques which are well known in the art. Each layer preferably has a thickness in the range of about 10 to about 500 Angstroms, with the preferred thickness range being from about 20 to about 200 Angstroms. The epitaxial deposition of the layers on the substrate is preferably conducted in an ultra-high vacuum system at a temperature in the range from about 350°C to about 800°C. In order to form the epitaxial layer in desired areas on the buffer layer, either the epitaxial layer can be selectively grown or, preferably, a full epitaxial layer is formed and then lithographically etched by well-known techniques.

For example, a photoresist layer may be laid down on the surface of the epitaxial layer. The photoresist layer is imagewise exposed to ultraviolet radiation through a mask and developed. The exposed areas are then removed leaving a positive photoresist image on the surface of the epitaxial layer. By removing the layer underlying exposed portions of the photoresist composition, corresponding portions of the epitaxial layer are uncovered. The uncovered epitaxial layer areas are then etched away. Then the balance of the photoresist is removed.

On the epitaxial layer a first electrical contact is deposited. On the buffer layer, but isolated from the epitaxial layer, is a second electrical contact. Optionally, on the opposite side of the substrate is a third electrical contact. Each of these contacts may comprise a suitable refractory metal: for example, aluminum, gold, silver, titanium, tungsten, molybdenum or an alloy thereof, among others. Each of the electrical

contacts may be applied by any convenient method including epitaxial deposition, sputtering or e-beam gun. The electrical contacts typically have a thickness ranging from about 100 Angstroms to about 250 Angstroms. The first, second and third contacts may be ohmic, Schottky or diffused contacts.

3.0 DEVICE OPERATION

In operation, the device is connected in an electric circuit, such as a tank circuit, wherein the first electrical contact is forward biased with a D.C. voltage of from about 0.1 to about 5 volts, preferably about 0.2 volt. The second electrical contact is reverse biased with a D.C. voltage. In the preferred embodiment, the third electrical contact is grounded.

A forward biased active region is a critical condition for operation of the device. Forward biasing of the first electrical contact junction injects minority charge carriers (i.e., thermionic emission) into the epitaxial layer and energizes initially encountered valence charge carriers in the epitaxial and buffer layers. A multiplication of charged carriers, such as electrons, energized by encounters with initially energized charge carriers diffuse toward the second electrical contact, in a sufficient quantity to establish a current. The second electrical contact junction, which is reverse biased, attracts these charge carriers and sweeps them out of the device. Once a resonance peak is reached, a self-induced regular oscillation commences since not only are charge carriers injected from the first electrical contact into the epitaxial layer, but a reverse stream of carriers may flow back to the first electrical contact.

Because of the high saturation velocity of the epitaxial layer, charge carriers move back and forth quickly, i.e., at frequencies up to and including terahertz frequencies. The use of a highly or linearly graded doped buffer layer to separate the second electrical contact from the epitaxial layer (and the first electrical contact) serves to alleviate contact resistivity, and hence thermal degeneration, by lowering the Schottky barrier height which the charge carriers must overcome. It is within the ability of the skilled artisan to tailor contact resistivity by varying the level of doping in the buffer layer. In the preferred embodiment, the third electrical contact is used either to establish yet another electron flow path to a separate circuit or to ground. Grounding is preferred to establish an optimum operating environment for the device by eliminating current leakage, body effect spurious currents, and buildup of heat in the substrate which reduces device efficiency.

The device is preferably connected in a tank circuit which receives the oscillating signal, maintains its frequency, amplifies it and uses it to calibrate a higher efficiency structure such as a microwave millimeter wave monolithic integrated circuit (MIMIC) for use in a radar receiver, logic device, burglar/proximity alarm system, BC detector or secure communication module.

4.0 EXAMPLE

1. LARGE SIGNAL OPERATING FREQUENCY

$$f = \frac{0.75 \cdot v_S}{L}$$

2. FLAT BAND VOLTAGE

$$V_{FB} = \frac{e \cdot N \cdot L^2}{2 \cdot \varepsilon}$$

3. REACH THROUGH VOLTAGE

$$V_{RT} = \frac{e \cdot N \cdot L^2}{2 \cdot \varepsilon} - L \cdot \left[2 \cdot e \cdot \frac{N}{\varepsilon} \cdot \left(V_{bi} - V_1 \right) \right]^{\frac{1}{2}}$$

4. MAXIMUM ELECTRIC FIELD ($E = dV_{FB}/dL$)

$$E_{MAX} = \frac{e \cdot N \cdot L}{\varepsilon}$$

5. BUILT IN POTENTIAL

$$V_{bi} = 25.9 \cdot 10^{-3} \cdot \ln\left(\frac{N}{n_i} \right)$$

6. JUNCTION CAPACITANCE

$$C = \frac{\varepsilon \cdot A}{L}$$

TABLE 1: Material Parameters

MATERIAL	v_{sat} (cm/s)	L (cm)	$N_{D,A}$ (cm^{-3})	ε_s	n_i (cm^{-3})	A (cm^{-2})*
Si	1×10^7	10^{-5}	10^{17}	11.7	1.5×10^{10}	2×10^{-11}
GaAs	2×10^7	10^{-5}	10^{17}	12.5	1.8×10^6	2×10^{-11}
GaN	2.5×10^7	10^{-5}	10^{17}	9.5	2.0×10^{10}	2×10^{-11}

* - assumes 5:1 aspect ratio

TABLE 2: Calculated Device Parameters

MATERIAL	f(THz)	V_{FB} (v)	V_{RT} (v)	V_{bi} (v)	E_{MAX} (x 10^5 v/cm)	C (fF)
Si	0.750	.773	-.027	.407	1.54	2.10
GaAs	1.500	.723	-.407	.641	1.44	2.21
GaN	1.875	.952	+.079	.400	1.90	1.68

It can be seen from the calculated results (Table 2) that a diode based on gallium nitride (GaN) demonstrates some promising performance specifications relative to frequency, (junction) capacitance and maximum electric field.

Let us now turn our attention to the current density versus voltage characteristics of the diode (Figure 2). This parameter will help to establish a baseline for the anticipated performance of the device. It can be seen that the GaN device operates comparable to the GaAs and better than the Si diode. When coupled with its superior material properties (wide energy band; high thermal conductivity), the GaN diode affords a robust device breakthrough in a mature, well understood device package.

$$J(V) := \left(2 \cdot \varepsilon \cdot \frac{v_S}{L^2}\right) \cdot$$

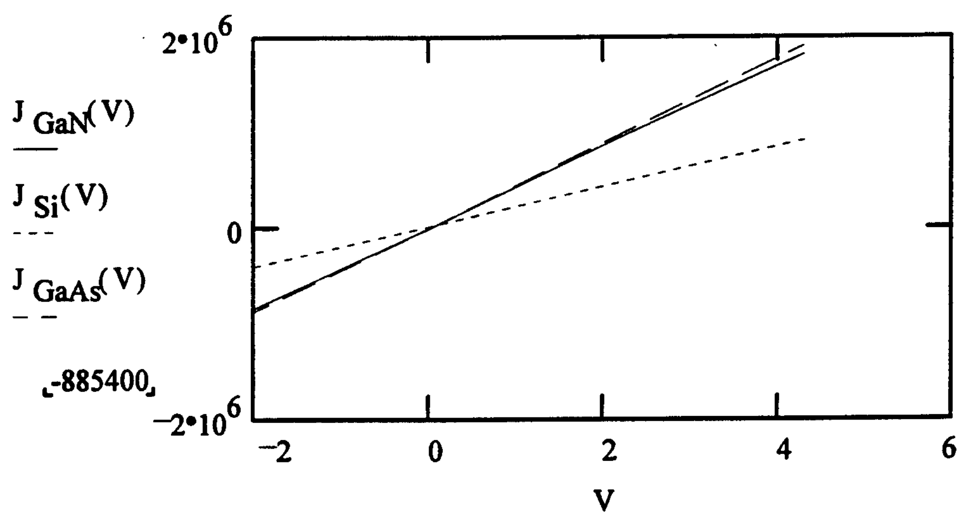

Figure 2. Diode Current Density vs. Voltage

5.0 CONCLUSIONS

It has been shown that devices operating into the terahertz range can be achieved using a new class of semiconductor materials applied to transit time device theory. Properties of these devices include higher breakdown fields and lower junction capacitances. While these devices possess historic low efficiencies (< 7%), their inclusion into a larger circuit, as a local oscillator, affords the ability to calibrate higher efficiency devices (i.e., MIMIC's) at terahertz frequencies. A realization of such devices would impact radar receiver, logic device, burglar/proximity alarm system, BC detector and secure communication module applications.

BIBLIOGRAPHY

1. S. M. Sze, Physics of Semiconductor Devices, John Wiley and Sons, 1981.

2. C. M. Wolfe et al., Physical Properties of Semiconductors, Prentice Hall, 1989.

3. E. S. Yang, Microelectronic Devices, McGraw Hill, 1988.

4. P. Das, D. K. Ferry, Journal of Solid State Electronics, Vol. 19, pp. 851-855, March 1976.

5. D. K. Ferry et al., Proceedings of 1st International Conference on GaN and Related Materials, Boston, MA, 1995.

6. D. K. Ferry, Physical Review B, Vol. 12, Number 6, pp. 2361-2369, 15 September 1975.

7. K.T. Tsen, Proceedings of MRS 1996 Fall Meeting, October 1996 (preprint).

8. W. A. Harrison, Solid State Theory, Dover Publications, 1979.

9. F. Seitz, The Modern Theory of Solids, Dover Publications, 1987.

10. W. Jones & N. H. March, Theoretical Solid State Physics, John Wiley & Sons, 1983.

11. S. Liao, Microwave Devices and Circuits, Prentice Hall, 1990.

12. K. K. Ng, Complete Guide to Semiconductor Devices, McGraw Hill, 1995.

13. R. H. Wittstruck, Method for High Frequency Device Operation with High Temperature and Radiation Hard Characteristics, U.S. Patent Application Serial No. 8 / 670,055, filed July 22, 1996.

ARMY RESEARCH LABORATORY
PHYSICAL SCIENCES DIRECTORATE
MANDATORY DISTRIBUTION LIST

Defense Technical Information Center*
ATTN: DTIC-OCC
8725 John J. Kingman Rd, STE 0944
Fort Belvoir, VA 22060-6218
(*Note: Two DTIC copies will be sent
from STINFO office, Ft Monmouth, NJ)

Director
US Army Material Systems Analysis Actv
ATTN: DRXSY-MP
(1) Aberdeen Proving Ground, MD 21005

Commander, AMC
ATTN: AMCDE-SC
5001 Eisenhower Ave.
(1) Alexandria, VA 22333-0001

Director
Army Research Laboratory
ATTN: AMSRL-D (John W. Lyons)
2800 Powder Mill Road
(1) Adelphi, MD 20783-1197

Director
Army Research Laboratory
ATTN: AMSRL-DD (COL Thomas A. Dunn)
2800 Powder Mill Road
(1) Adelphi, MD 20783-1197

Director
Army Research Laboratory
2800 Powder Mill Road
Adelphi, MD 20783-1197
(1) AMSRL-OP-SD-TA (ARL Records Mgt)
(1) AMSRL-OP-SD-TL (ARL Tech Library)
(1) AMSRL-OP-SD-TP (ARL Tech Publ Br)

Directorate Executive
Army Research Laboratory
Physical Sciences Directorate
Fort Monmouth, NJ 07703-5601
(1) AMSRL-SE
(1) AMSRL-SE-C (V. Rosati)
(1) AMSRL-SE-C (M. Hayes)
(1) AMSRL-OP-FM-RM
(22) Originating Office

Advisory Group on Electron Devices
ATTN: Documents
Crystal Square 4
1745 Jefferson Davis Highway, Suite 500
(2) Arlington, VA 22202

Commander, CECOM
R&D Technical Library
Fort Monmouth, NJ 07703-5703
(1) AMSEL-IM-BM-I-L-R (Tech Library)
(3) AMSEL-IM-BM-I-L-R (STINFO Ofc)

Deputy for Science & Technology
Office, Asst Sec Army (R&D)
(1) Washington, DC 20310

HQDA (SARDA-TR)
Dr. Richard Chait
(1) Washington, DC 20310

Director
Naval Research Laboratory
ATTN: Code 2627
(1) Washington, DC 20375-5000

USAF Rome Laboratory
Technical Library, FL2810
ATTN: Documents Library
Corridor W, STE 262, RL/SUL
26 Electronics Parkway, Bldg 106
Griffiss Air Force Base
(1) NY 13441-4514

Dir, ARL Battlefield
Environment Directorate
ATTN: AMSRL-BE
White Sands Missile Range
(1) NM 88002-5501

Dir, ARL Sensors, Signatures,
Signal & Information Processing
Directorate (S3I)
ATTN: AMSRL-SS
2800 Powder Mill Road
(1) Adelphi, MD 20783-1197

Dir, CECOM Night Vision/
Electronic Sensors Directorate
ATTN: AMSEL-RD-NV-D
(1) Fort Belvoir, VA 22060-5806

Dir, CECOM Intelligence and
Electronic Warfare Directorate
ATTN: AMSEL-RD-IEW-D
Vint Hill Farms Station
(1) Warrenton, VA 22186-5100

Cdr, Marine Corps Liaison Office
ATTN: AMSEL-LN-MC
(1) Fort Monmouth, NJ 07703-5033